AGU PUBLICATIONS

Geophysical Research Letters

RESEARCH LETTER
10.1002/2015GL066009

Key Points:
- fCO_2 and air-sea flux of CO_2 strongly modulated by intraseasonal variability in the SO
- Uncertainty of the mean seasonal or annual air-sea flux is sensitive to sampling resolution
- A sampling resolution <2 days is necessary in 30–40% of the SO to reduce the uncertainty to <10%

Supporting Information:
- Supporting Information S1

Correspondence to:
P. M. S. Monteiro,
pmonteir@csir.co.za

Citation:
Monteiro, P. M. S., L. Gregor, M. Lévy, S. Maenner, C. L. Sabine, and S. Swart (2015), Intraseasonal variability linked to sampling alias in air-sea CO_2 fluxes in the Southern Ocean, *Geophys. Res. Lett.*, *42*, 8507–8514, doi:10.1002/2015GL066009.

Received 1 SEP 2015
Accepted 23 SEP 2015
Accepted article online 28 SEP 2015
Published online 21 OCT 2015

Intraseasonal variability linked to sampling alias in air-sea CO_2 fluxes in the Southern Ocean

Pedro M. S. Monteiro[1,2], Luke Gregor[1,2], Marina Lévy[3], Stacy Maenner[4], Christopher L. Sabine[4], and Sebastiaan Swart[1,2]

[1]Southern Ocean Carbon - Climate Observatory, CSIR, Rosebank, South Africa, [2]Department of Oceanography, University of Cape Town, Rondebosch, South Africa, [3]Sorbonne Université (UPMC, Paris 6)/CNRS/IRD/MNHN, Laboratoire d'Océanographie et du Climat, Institut Pierre, Simon Laplace, Paris, France, [4]NOAA/PMEL, Seattle, Washington, USA

Abstract The Southern Ocean (SO) contributes most of the uncertainty in contemporary estimates of the mean annual flux of carbon dioxide CO_2 between the ocean and the atmosphere. Attempts to reduce this uncertainty have aimed at resolving the seasonal cycle of the fugacity of CO_2 (fCO_2). We use hourly CO_2 flux and driver observations collected by the combined deployment of ocean gliders to show that resolving the seasonal cycle is not sufficient to reduce the uncertainty of the flux of CO_2 to below the threshold required to reveal climatic trends in CO_2 fluxes. This was done by iteratively subsampling the hourly CO_2 data set at various time intervals. We show that because of storm-linked intraseasonal variability in the spring-late summer, sampling intervals longer than 2 days alias the seasonal mean flux estimate above the required threshold. Moreover, the regional nature and long-term trends in storm characteristics may be an important influence in the future role of the SO in the carbon-climate system.

1. Introduction

The Southern Ocean (SO), south of the Sub-Tropical Front (STF), contributes 50% (~1 Pg C yr^{-1}) of the total ocean uptake of anthropogenic CO_2 and is the main source of uncertainty in empirical and model-based estimates of the mean annual CO_2 fluxes between the ocean and the atmosphere [*Landschützer et al.*, 2014; *Lenton et al.*, 2013; *Lovenduski et al.*, 2015; *Majkut et al.*, 2014; *Matear and Lenton*, 2008; *Takahashi et al.*, 2012]. Climate sensitivities of CO_2 ocean-atmosphere exchange (FCO_2) and storage in the SO are increasingly recognized as one of the major sources of uncertainty in the century-scale projections of atmospheric CO_2 and associated long-term climate adjustments that lead to climate change [*Anav et al.*, 2013; *Fay and McKinley*, 2013; *Fay et al.*, 2014; *Gruber et al.*, 2009; *Hauck et al.*, 2013; *Le Quéré et al.*, 2009; *Sabine et al.*, 2004; *Wanninkhof et al.*, 2013]. Resolving interannual variability and trends in the air-sea CO_2 flux in the SO will contribute to reducing both the magnitude of the uncertainty of CO_2 fluxes and provide a better understanding of the climate sensitive dynamics that drive them [*Fay and McKinley*, 2013; *Landschützer et al.*, 2014; *Majkut et al.*, 2014]. The paucity of observations, limitations around biogeochemical model dynamics and uncertainties linked to model-scale sensitivities in the SO still present major challenges to ocean climate research goals to resolve interannual variability of CO_2 fluxes [*Landschützer et al.*, 2014; *Le Quéré et al.*, 2014; *Lenton et al.*, 2013; *Majkut et al.*, 2014; *Resplandy et al.*, 2014; *Rödenbeck et al.*, 2013].

Reducing this uncertainty to <10% (<0.1 Pg C yr^{-1}) of its mean annual net uptake of CO_2 is critical to resolving interannual variability and trends of FCO_2 in the Southern Ocean [*Landschützer et al.*, 2014; *Majkut et al.*, 2014; *Monteiro et al.*, 2010]. This is particularly urgent in the context of the strengthening of the nonsteady state dynamics of natural and anthropogenic ocean carbon resulting from climate-linked changes in ocean physics and carbonate chemistry [*Le Quéré et al.*, 2007; *McNeil and Matear*, 2013].

Resolving the seasonal bias of observations in the SO—there are far fewer in winter—is considered a major challenge in reducing the uncertainty in the mean annual fluxes and resolving the seasonal cycle is considered a first-order contribution to reducing the uncertainty of the mean annual CO_2 flux [*Landschützer et al.*, 2014; *Lenton et al.*, 2012; *Majkut et al.*, 2014; *Monteiro et al.*, 2010; *Takahashi et al.*, 2009]. However, to date, most of the effort in sustained CO_2 observations in the SO have been ship based contributing in a coordinated approach to a global gridded data set [*Bakker et al.*, 2012; *Pfeil et al.*, 2013; *Sabine et al.*, 2013]. Ships alone are not able to adequately resolve the seasonal cycle due to the operational limitations of the required

sampling frequency: quarterly circumpolar meridional lines with a 30° interval [*Monteiro et al.*, 2010; *Lenton et al.*, 2006]. High temporal resolution Lagrangian drifting buoy studies have also contributed to both constraining the basin-scale mean seasonal cycle along their trajectories and pointing to the potential role of fine-scale dynamics [*Boutin et al.*, 2008; *Resplandy et al.*, 2014]. Models have been used to close the spatial and temporal data sparseness of existing ship-based observations, particularly in the most recent Regional Carbon Cycle Assessment and Processes (ReCCAP) assessment of global and regional trends in ocean-atmosphere CO_2 flux assessments [*Lenton et al.*, 2013]. However, while inverse, coupled ocean biogeochemical models and Coupled Model Intercomparison Project Phase 5 models show adequate (-0.42 ± 0.07) agreement on the mean annual FCO_2 in the SO, they disagree on the phasing and amplitude of the seasonal cycle [*Lenton et al.*, 2013; *Anav et al.*, 2013]. This raises questions about the scale sensitivity of process dynamics in global models and their own limits in terms of reducing uncertainties and predicting trends of the mean annual CO_2 fluxes.

Most recently, the challenge of reducing the uncertainty of the mean annual flux of CO_2 in the SO by fully resolving the seasonal cycle is being addressed through observational and empirical modeling approaches where the sparseness and variability of the data are captured by proxy variables [*Landschützer et al.*, 2014; *Majkut et al.*, 2014; *Rödenbeck et al.*, 2013]. An ocean model-based set of observational-system simulation experiments showed that monthly observations from 200 profiling floats could resolve the seasonal cycle across the SO and reduce the uncertainty of the mean annual CO_2 flux to < 0.1 Pg C yr^{-1} [*Landschützer et al.*, 2014]. These studies are reducing the uncertainties in seasonally resolved annual fluxes and starting to characterize interannual and decadal variability from long-term trends in the CO_2 fluxes in the SO [*Fay et al.*, 2014; *Landschützer et al.*, 2014; *Le Quéré et al.*, 2007; *Rödenbeck et al.*, 2013]. However, an additional source of uncertainty could arise from the subsampling of a highly varying system, which can alias the mean fluxes. A model study applied to the midlatitude Mediterranean Sea has suggested that the sampling period must be no greater than a few days to estimate the CO_2 flux with less than 20% error [*Mémery et al.*, 2002].

Here we use an unprecedented quasi-fixed location high-resolution data set from a robotic glider-based experiment to examine whether resolving the seasonal cycle is sufficient to meet the uncertainty threshold in a highly variable part of the SO. We show how the mean seasonal air-sea fugacity (fCO_2) and flux (FCO_2) of CO_2 are sensitive to intraseasonal modes of variability and consequently how error and biases of their mean are sensitive to the sampling period. In our study the use of intraseasonal refers to variability modes spanning synoptic to subseasonal scales.

2. Materials and Methods

The 4 month long second Southern Ocean Seasonal Cycle Experiment (SOSCEx II) was set in the Sub-Antarctic Zone (SAZ), here defined as the zone between the Sub-Antarctic and Sub-Tropical fronts, approximately 1300 km SW of Cape Town (Figure 1 and Figures S1a–S1c in the supporting information). These spatiotemporally high-resolution (hourly and 1 km) observations were obtained from a simultaneous deployment of a Liquid Robotics Wave Glider outfitted with a surface CO_2 sensor modified from a MAPCO2 system [*Sutton et al.*, 2014] and a profiling buoyancy glider (Figures S1a–S1c). The gliders were deployed at 41°S, 9.5°E on 13 October 2013 and navigated to a pseudomooring circular sampling pattern with a diameter of 16 km, centered at 43°S, 8.5°E where they arrived on 17 November 2013. The experiment was terminated on 8 February 2014. This MAPCO2 system achieves a precision of < 2 μatm for seawater pCO_2 [*Sutton et al.*, 2014]. Air-sea CO_2 fluxes were calculated from in situ air and sea pCO_2, temperature, and salinity measurements and scatterometer winds (http://podaac.jpl.nasa.gov) using the *Nightingale et al.* [2000] formulation.

To assess the sensitivity of the seasonal mean to the sampling period, the hourly air-sea CO_2 gradient (ΔfCO_2) and air-sea flux of CO_2 (FCO_2) time series (Figure 2a) were sampled over a continuous range of intervals from hourly to monthly (Figures 2b and 2c). In order to obtain many realizations of a mean, the starting time was shifted iteratively by an hour for each sampling interval. This means that a 2 h interval would return two mean values and sampling every 3 days (72 h) resulted in 72 possible mean values. These mean values for various sampling intervals were plotted as a two-dimensional histogram (bin resolution of 0.5 days and 2 μmol m^{-2} h^{-1}). Bins were normalized by the number of bins for each sampling interval to show the percentage likelihood of achieving a particular observation (right-hand axis in Figures 2b and 2c).

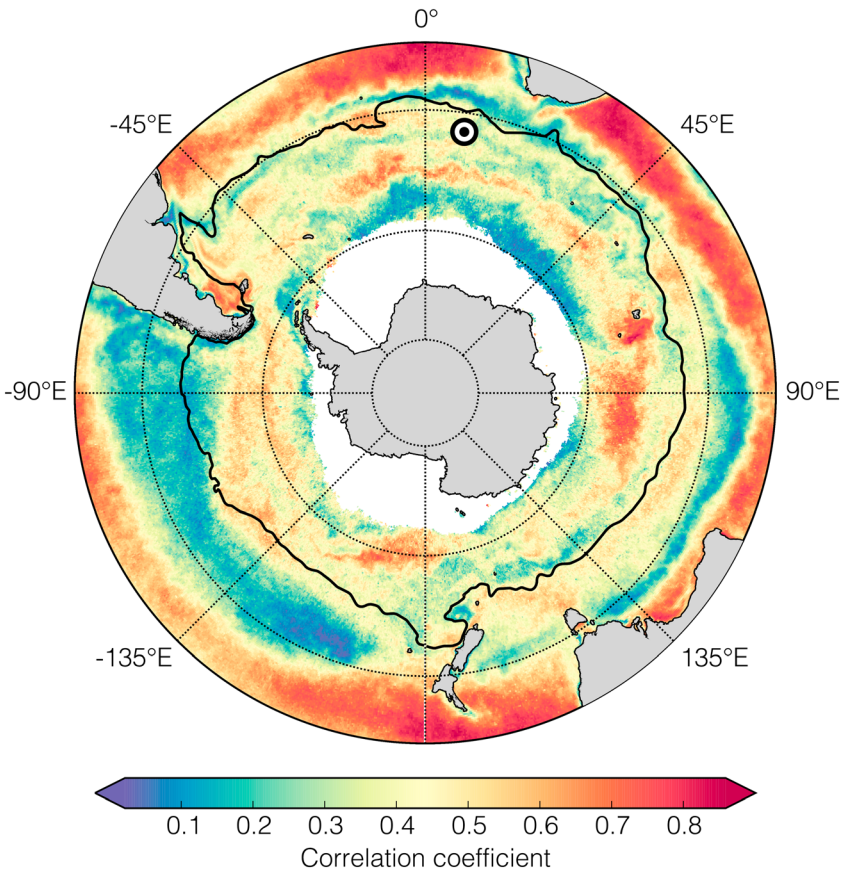

Figure 1. The sampling location for SOSCEx II (black-white dot) was in a region of intraseasonal dynamics in the Sub-Antarctic Zone south of Africa and that these characteristics extend over at least 30% of the area of the Southern Ocean. The mean positions of the Sub-Tropical Front (STF) and the Polar Front (PF) are depicted over the spatial characteristics of the correlation of the seasonal cycle (1998–2007) with the decadal mean of the seasonal cycle of satellite chlorophyll *a*. Areas of low correlation ($r^2 < 0.4$: low seasonal cycle reproducibility) are dominated by intraseasonal dynamics and a high correlation coefficient ($r^2 > 0.4$: high seasonal cycle reproducibility) are characterized by a seasonal cycle reproducible interannually.

In order to generalize our results to the Southern Ocean, we adopted a methodology that linked the sampling scale error that emerged from our data at the SAZ sampling location (Figures 2b and 2c) to the Chl *a*-based seasonal cycle reproducibility correlation (r^2) in Figure 1. The details of this methodology and all its assumptions are outlined in the supporting information Text S3. This methodology was used to generate a SO-scale plot of the spatial distribution of the mean sampling error based on a uniform 10 day sampling period (Figure 4).

3. Results and Discussion

3.1. Spatial Extent of Intraseasonal Variability in the Southern Ocean

The large spatial scale extent of intraseasonal modes of variability in the Southern Ocean is highlighted in Figure 1. It depicts the correlation (r^2), termed the seasonal cycle reproducibility for satellite chlorophyll *a* (Chl *a*). It is the fraction of the overall variance for the period 1998–2007 that is explained by the mean seasonal cycle [*Thomalla et al.*, 2011]. Areas with $r^2 > 0.4$ are characterized as having high seasonal cycle reproducibility and those where $r^2 < 0.4$, low seasonal cycle reproducibility (Figure 1). In the latter the variability is dominated by intraseasonal (largely storm driven) modes [*Carranza and Gille*, 2015; *Swart et al.*, 2014]. It shows that intraseasonal variability is a characteristic of large areas of the SAZ and in the vicinity of the ice edge. Here we only use Chl *a* as a proxy for areas where CO_2 may also be exposed to comparatively high-frequency forcing because both have been found to be modulated by storm forcing [*Swart et al.*, 2014; *Thomalla et al.*, 2011] for Chl *a* and this study for CO_2. Based on these plots we estimate the area in which

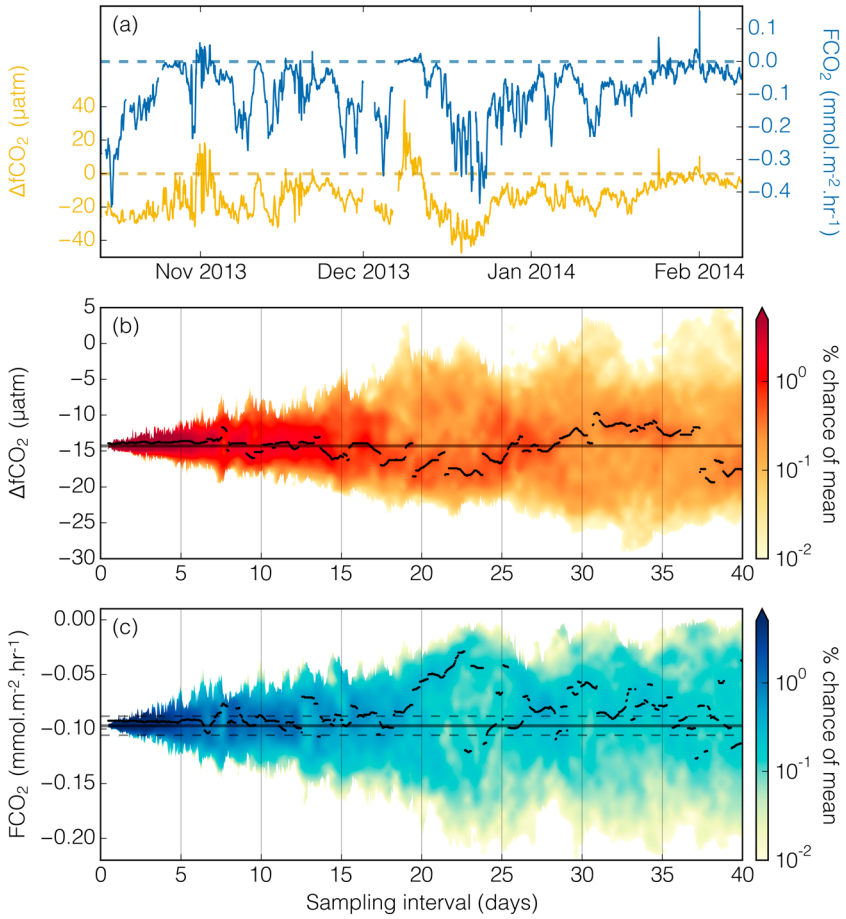

Figure 2. (a) 4 month time series of observed ΔfCO_2 (μatm) and derived fluxes FCO_2 (mmol C m^{-2} h^{-1}) from the SOSCEx II sampling location in the SAZ. It shows the strong intraseasonal modes and highlights important differences in the intraseasonal timing between the two variables. (b and c) The sensitivity of the sampling means of ΔfCO_2 (Figure 2b) and FCO_2 (Figure 2c) to the sampling interval (period). The widening ranges indicate how, in systems characterized by strong intraseasonal variability, the uncertainty in the mean seasonal ΔfCO_2 and FCO_2 increase as the sampling frequency decreases. The dashed lines represent the 10% uncertainty threshold on either side of the hourly data mean, and the broken solid line depicts the variability of the mode. It shows (right-hand scale) that the probability of achieving the accurate hourly sampling mean falls rapidly with increasing sampling period to $<1\%$ above a 10 day period.

the annual seasonal cycle is dominated by intraseasonal modes to cover 30–40% of the SO Southern Ocean south of the STF.

Surface carbon (fCO_2 and FCO_2) and water column physics variables for the full hourly sampled time series show that there are a variety of strong intraseasonal (1–10 days) modes of variability (Figure 2a). This time scale corresponds to that of atmospheric storms passing over the gliders [*Swart et al.*, 2014]. The intraseasonal variability ranges from strong ingassing fluxes of −0.1 to −0.45 mM m^{-2} h^{-1} (equivalent to −2.4 to −10.8 mM m^{-2} d^{-1}) to near-zero magnitude fluxes and short periods of strong outgassing air-sea fCO_2 gradients (ΔfCO_2) but weak outgassing fluxes. (Figure 2a) The seasonal means for ΔfCO_2 and FCO_2 from the hourly data over the 4 month period are −14.5 μatm and −2.3 mM C m^{-2} d^{-1}, respectively (Table 1). We now examine the question of whether subsampling over a range of periods creates a systematic alias of these means.

3.2. Sampling Period Sensitivities

The relationship between sampling period and uncertainty in the means is depicted for fCO_2 and FCO_2 in Figures 2b and 2c. The wider the spread of means, the lower the probabilities of achieving a particular mean (Figures 2b and 2c). If each seasonal mean were insensitive to the sampling period, then the magnitudes would remain close to the hourly based mean over the range of periods (Figures 2b and 2c).

Table 1. Summary of the Increasing Uncertainty Ranges of the Means at Three Widely Used Sampling Periods[a]

Sampling Period	ΔfCO_2			FCO_2		
Days	Mean	5th Percentile	95th Percentile	Mean	5th Percentile	95th Percentile
1	−14.3	−0.6	+0.9	−2.3	−0.12	+0.15
10	−14.3	−2.8	+4.2	−2.3	−0.66	+0.64
30	−14.3	−10.6	+11.4	−2.3	−1.77	+1.08

[a]It compares the absolute mean seasonal ΔfCO_2 and FCO_2 for the hourly high-resolution data set with the magnitudes of the ranges at the 5th and 95th percentiles. It contrasts the $<10\%$ uncertainty at 1 day period with $>75\%$ uncertainty at monthly periods.

Three notable features are revealed by Figures 2b and 2c: first, for both ΔfCO_2 and FCO_2 the range of the sampling means, a measure of the uncertainty, increases sharply from daily to 10 daily to monthly sampling frequencies (see also Table 1). Expressed statistically, the likelihood of returning the hourly sampled mean decreases rapidly from $>50\%$ at <5 day periods to $<1\%$ at >10 day frequencies. Second, and from a perspective of reducing the uncertainty of the mean annual FCO_2, a more serious problem, is the uncertainty in the magnitude of the biases that emerge (Figures 2b and 2c). At certain sampling periods, the probability of returning a mean that is significantly different to the hourly mean is larger, which would result in not just increased uncertainty but also a bias. This is seen for both ΔfCO_2 and FCO_2 where higher probabilities occur above or below the hourly mean (Figures 2b and 2c). Third, the percent contribution of the increasing uncertainty associated with decreasing sampling frequencies is greater for the FCO_2 than for ΔfCO_2 (see also Table 1). For ΔfCO_2 and FCO_2 the range of sampling means, our absolute measure of uncertainty or observational error, increases from a minimum of ±5% of the hourly based data mean at daily resolution to ±20% (ΔfCO_2) and ±50% (FCO_2) in the 10 day period and ±75% (ΔfCO_2) and ±100% (FCO_2) in the monthly sampling period range (Table 1 and Figures 2b and 2c). That is, FCO_2 is more sensitive to the sampling period than ΔfCO_2. We now examine the basis for these differences.

3.3. Differences in Intraseasonal Variability of Air-Sea CO_2 Gradients and Fluxes

The explanation for the differences in the sampling period sensitivities for fCO_2 and FCO_2 is that the intraseasonal periods of variability are different: the longer ΔfCO_2 period is determined by the phasing of the phytoplankton bloom dynamics and storm-driven entrainment of subsurface dissolved inorganic carbon (DIC), whereas the shorter FCO_2 is modulated by the phasing of the wind and the entrainment of DIC (Figure 3). The mechanistic basis for the differences in aliases between ΔfCO_2 and FCO_2 is synthesized in Figure 3 as a single idealized event. It shows that the contrasting modal characteristics for ΔfCO_2 and FCO_2 arise from differences in the phasing of the two main drivers of the flux of CO_2: primary productivity (2), which affects DIC and ΔfCO_2 and wind stress (1), which affects both the magnitude of the flux as well as the entrainment of subthermocline high-DIC waters (8). The period of the ΔfCO_2 mode is initiated by the intraseasonal bloom event (2), which rapidly strengthens a negative disequilibrium relative to the atmosphere (3). During this phase the flux (grey) remains weak or zero because the low wind stress (4) and the intraseasonal bloom (2) are out of phase. The ingassing flux only strengthens (5) and peaks (6) late in the ΔfCO_2 cycle when the next synoptic storm event (4) increases the wind stress. However, strong magnitude storms not only enhance air-sea gas exchange but also deepen the mixed layer depth, entraining subpycnocline DIC (7, 8). In a CO_2 sink region such as the SAZ, DIC entrainment rapidly weakens ΔfCO_2, which weakens the flux even though the wind stress may remain high (7, 8). The net effect of the phase difference between the intraseasonal bloom and synoptic wind stress is that ΔfCO_2 and FCO_2 have different periods with the latter being significantly shorter (1–3 days) than the former (5–8 days). The aliases between ΔfCO_2 and FCO_2 seasonal means then develop as a result of the extent to which fine-scale (<2 days) and coarse-scale (>10 days) samplings resolve these contrasting intraseasonal CO_2 modes.

This conceptual model is supported by a wavelet analysis of ΔfCO_2 and FCO_2 time series, which shows that the latter has high-frequency modes of <2 days, which are largely absent in the ΔfCO_2 data set (Figures S3a and S3b in the supporting information). Sampling ΔfCO_2 as opposed to FCO_2 lessens the error significantly (by about half), but the greater sensitivity of FCO_2 to sampling error highlights that it is critical to also resolve the synoptic scale of the wind stress in order not to overestimate the magnitude of the fluxes derived from

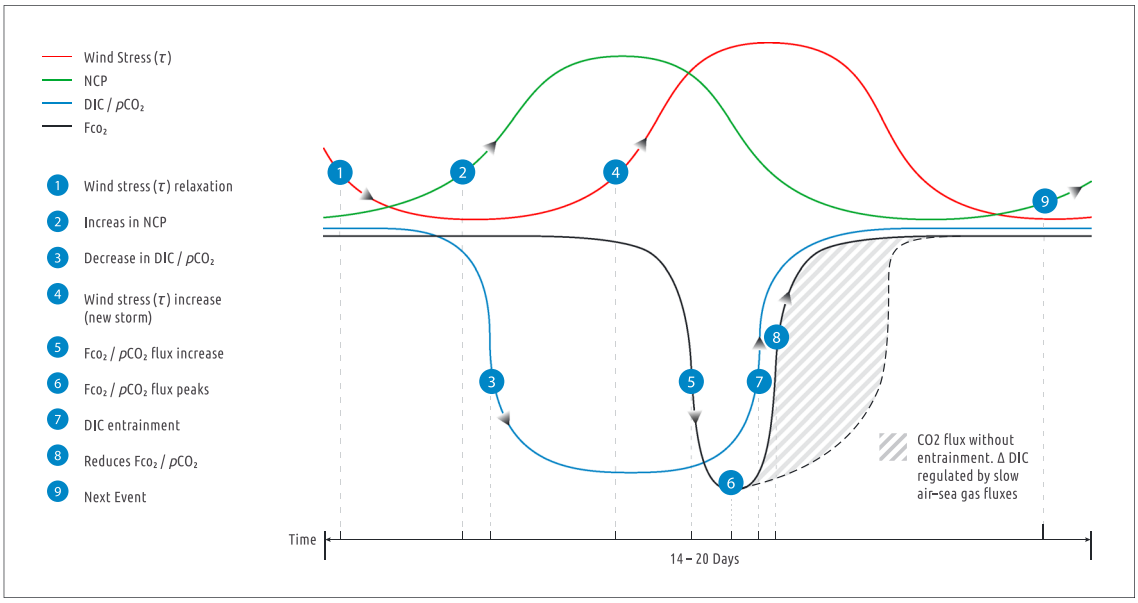

Figure 3. A schematic showing how differences in the phasing of the intraseasonal scales in wind and phytoplankton blooms lead to differences in the sensitivities of ΔfCO_2 and FCO_2 to sampling frequency. FCO_2 has a shorter intraseasonal period than ΔfCO_2 (see text).

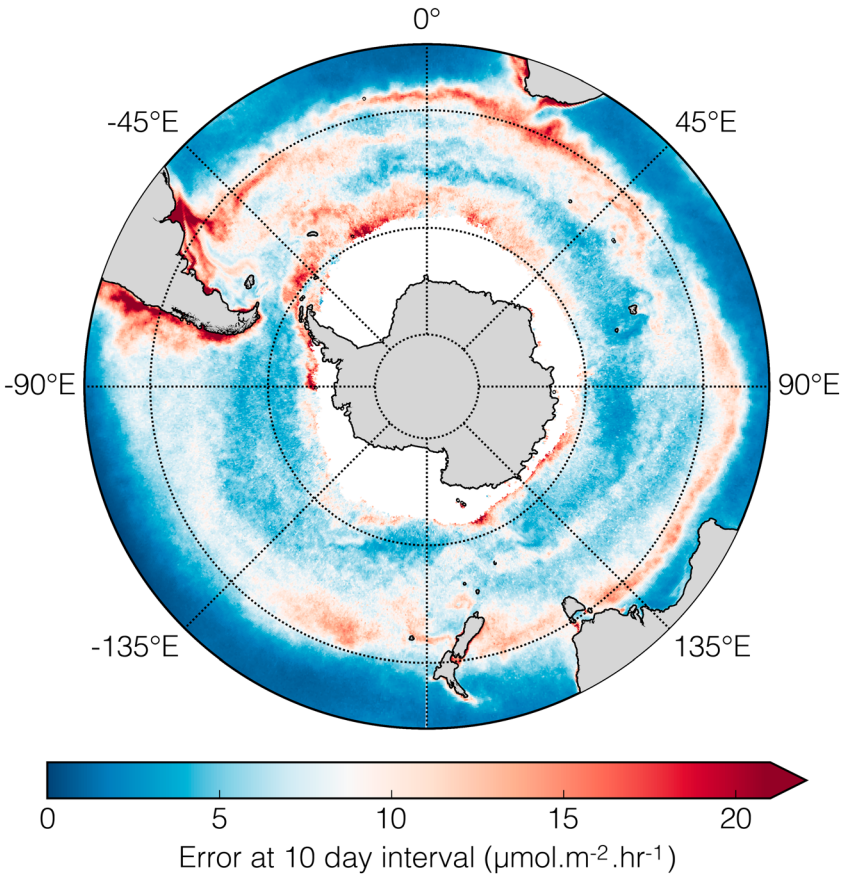

Figure 4. (a) The spatial variability of the FCO_2 uncertainties, which arise from a uniform 10 day sampling period choice. The Southern Ocean is characterized with uncertainties of 10–25% (10–25 $\mu mol\ m^{-2}\ h^{-1}$) at this sampling period.

observed ΔfCO_2. In other words, the synoptic period and the spatial scale of the wind stress, particularly the magnitude and phasing of storm events, make a significant contribution to reducing the uncertainty of the flux.

This finding highlights that efforts to reduce the uncertainty of FCO_2 in the SO by resolving the seasonal cycle will not be sufficient to reduce the uncertainty to below 10% of the mean annual flux or <0.1 Pg C yr^{-1} required to resolve interannual variability and trends [*Lenton et al*., 2006; *Monteiro et al*., 2010; *Landschützer et al*., 2014; *Majkut et al*., 2014]. We show that daily to 2 day period observations are essential in regions of high intraseasonal variability, such as the SAZ, and the Marginal Ice Zone if an uncertainty of <10% is to be achieved in this important part of the global ocean carbon cycle. These sampling frequency sensitivities would apply only to regions of the SO characterized by intraseasonal variability (Figure 1) but also raise the need to further investigate the impact that these scales of variability have on global mean annual CO_2 fluxes and the regional biases that emerge from different basins. It also suggests that we need to have a sampling frequency strategy that is sensitive to the local characteristics of variability. An analysis using 0.5° resolution model with a 5 day resolution but sampled at 15 day intervals supports comparable results (see supporting information Text S5 and Figure S5).

3.4. Southern Ocean-Scale Observations Implications

We now propose a Southern Ocean-scale generalization of the significance of these findings by examining the large-scale impact of a fixed period (10 days) sampling strategy, typical for profiling floats on the uncertainty range of the air-sea flux of CO_2. (Figure 4). Here we use the correlation (r^2) ranges for seasonal cycle reproducibility depicted in Figure 1 and the flux uncertainties derived from our observations in Figures 2b and 2c (methodology described in the supporting information). It shows that based on a mean seasonal flux of ~0.095 mmol C m^{-2} h^{-1}, derived from the hourly data set, a uniform 10 day sampling period results in uncertainties in the range of 10–25% over much of the SO (Figure 4 and Table 1). The plot points to the SAZ and the marginal ice zone as being regions where the sampling alias is most sensitive to high-frequency sampling or where the error at a sampling frequency of 10 days is highest (Figure 4). It is also notable that the Atlantic Ocean basin may be making the strongest contribution to sampling alias errors for the Southern Ocean (Figure 4).

As a corollary, we propose that a response to the error limitations, highlighted by a fixed period strategy typical of floats in Figure 4, may be a variable sampling period strategy (Figure S3). It shows that areas with a seasonal cycle reproducibility $r^2 < 0.5$ may only be resolved by sampling periods of 1–3 days, while in areas with high seasonal cycle reproducibility ($r^2 > 0.5$) sampling periods of 5–10 days are viable.

These plots do not aim to provide accurate estimates of the CO_2 flux sampling error sensitivity but rather should be considered as useful for illustrative purposes to further explain the discussion in the ocean CO_2 observations community that is initiated by our results. The objectives show that because of the heterogeneity of intraseasonal to seasonal modes of CO_2 fluxes in the SO, fixed period sampling strategies will not yield the required low uncertainties. This may be achieved by a scale sensitive adaptive sampling strategy (Figure S3).

4. Synthesis

In conclusion, our study shows that resolving the seasonal cycle is not sufficient to resolve interannual variability and trends in the flux of CO_2 in the SO. Planned expanded sampling strategies using ships and biogeochemical floats to minimize the uncertainty of $FCO_2 < 0.1$ Pg C yr^{-1} in the SO will not achieve their objectives unless they are able to use an adaptive sampling frequency ranging from 1 to 30 days depending on the region and the season. This applies especially in zones characterized by CO_2 intraseasonal dynamics, such as the Sub-Antarctic Zone and the Marginal Ice Zones where most of the CO_2 uptake and subsequent interior storage in the SO occurs. These findings also highlight an important climate sensitivity of the carbon cycle in the SO and comparable areas of the ocean in general to changes in the characteristics of buoyancy forcing and storms, both of which regulate the intraseasonal dynamics.

Acknowledgments
The authors acknowledge their institutional support (PM, LG, SS: CSIR Parliamentary Grant and Africa Centre for Earth Systems Science), CLS: PMEL contribution 4341, The Department of Science and Technology in South Africa for funding the robotic infrastructure and NRF for supporting this research (grant 80253). We also deeply appreciative of the support that SOSCEx II got from the Department of Environment Affairs through time on the logistics cruises of the R/V *S.A. Agulhas* II as well as its captain, officers, and crew. The fieldwork component would not have been possible without the support of the marine engineers and glider pilots at the CSIR's South African Marine Engineering and Robotics Centre (SAMERC) in partnership with Sea Technology Services. This paper is a contribution to EUFP7 projects SOCCLI (PIRSES-GA-2012-317699) and Carbochange (grant 264879). The Globcolour Project supplied the blended ocean color data. This CO_2 data will be made available through the Carbon Dioxide Information and Analysis Centre. We also thank Bianca Bird for drawing the conceptual model in Figure 3.

The Editor thanks two anonymous reviewers for their assistance in evaluating this paper.

References

Anav, A., P. Friedlingstein, M. Kidston, L. Bopp, P. Ciais, P. Cox, C. Jones, M. Jung, R. Myneni, and Z. Zhu (2013), Evaluating the land and ocean components of the global carbon cycle in the CMIP5 Earth system models, *J. Clim.*, *26*(18), 6801–6843, doi:10.1175/JCLI-D-12-00417.1.

Bakker, D. C. E., et al. (2012), Global data products help assess changes to the ocean carbon sink, *Eos Trans. AGU*, *93*(12), 125–126, doi:10.1029/2012EO120001.

Boutin, J., L. Merlivat, C. Henocq, N. Martin, and J. B. Sallee (2008), Air-sea CO_2 flux variability in frontal regions of the Southern Ocean from CARIOCA drifters, *Limnol. Oceanogr.*, *53*, 2062–2079.

Carranza, M. M., and S. T. Gille (2015), Southern Ocean wind-driven entrainment enhances satellite chlorophyll-*a* through the summer, *J. Geophys. Res., Oceans*, *120*, 304–323, doi:10.1002/2014JC010203.

Fay, A. R., and G. A. McKinley (2013), Global trends in surface ocean pCO_2 from in situ data, *Global Biogeochem. Cycles*, *27*, 541–557, doi:10.1002/gbc.20051.

Fay, A. R., G. A. McKinley, and N. S. Lovenduski (2014), Southern Ocean carbon trends: Sensitivity to methods, *Geophys. Res. Lett.*, *41*, 6833–6840, doi:10.1002/2014GL061324.

Gruber, N., et al. (2009), Oceanic sources, sinks, and transport of atmospheric CO_2, *Global Biogeochem. Cycles*, *23*, GB1005, doi:10.1029/2008GB003349.

Hauck, J., C. Völker, T. Wang, M. Hoppema, M. Losch, and D. A. Wolf-Gladrow (2013), Seasonally different carbon flux changes in the Southern Ocean in response to the southern annular mode, *Global Biogeochem. Cycles*, *27*, 1236–1245, doi:10.1002/2013GB004600.

Landschützer, P., N. Gruber, D. C. E. Bakker, and U. Schuster (2014), Recent variability of the global ocean carbon sink, *Global Biogeochem. Cycles*, *28*, 927–949, doi:10.1002/2014GB004853.

Le Quéré, C., et al. (2007), Saturation of the Southern Ocean CO_2 sink due to recent climate change, *Science*, *316*, 1735–1738, doi:10.1126/science.1136188.

Le Quéré, C., et al. (2009), Trends in the sources and sinks of carbon dioxide, *Nat. Geosci.*, *2*(12), 831–836, doi:10.1038/ngeo689.

Le Quéré, C., et al. (2014), Global carbon budget 2014, *Earth Syst. Sci. Data Discuss.*, *7*(2), 521–610, doi:10.5194/essd-6-235-2014.

Lenton, A., R. J. Matear, and B. Tilbrook (2006), Design of an observational strategy for quantifying the Southern Ocean uptake of CO_2, *Global Biogeochem. Cycles*, *20*, GB4010, doi:10.1029/2005GB002620.

Lenton, A., N. Metzl, T. Takahashi, M. Kuchinke, R. J. Matear, T. Roy, S. C. Sutherland, C. Sweeney, and B. Tilbrook (2012), The observed evolution of oceanic pCO_2 and its drivers over the last two decades, *Global Biogeochem. Cycles*, *26*, GB2021, doi:10.1029/2011GB004095.

Lenton, A., et al. (2013), Sea-air CO_2 fluxes in the Southern Ocean for the period 1990–2009, *Biogeosciences*, *10*, 4037–4054, doi:10.5194/bg-10-4037-2013.

Lovenduski, N. S., A. R. Fay, and G. A. McKinley (2015), Observing multidecadal trends in Southern Ocean CO_2 uptake: What can we learn from an ocean model?, *Global Biogeochem. Cycles*, *29*, 416–426, doi:10.1002/2014GB004933.

Majkut, J. D., B. R. Carter, T. L. Frölicher, C. O. Dufour, K. B. Rodgers, and J. L. Sarmiento (2014), An observing system simulation for Southern Ocean carbon dioxide uptake, *Philos. Trans. A. Math. Phys. Eng. Sci.*, *372*, doi:10.1098/rsta.2013.0046.

Matear, R. J., and A. Lenton (2008), Impact of historical climate change on the Southern Ocean carbon cycle, *J. Clim.*, *21*(22), 5820–5834, doi:10.1175/2008JCLI2194.1.

McNeil, B. I., and R. J. Matear (2013), The non-steady state oceanic CO_2 signal: Its importance, magnitude and a novel way to detect it, *Biogeosciences*, *10*, 2219–2228, doi:10.5194/bg-10-2219-2013.

Mémery, L., M. Lévy, S. Vérant, and L. Merlivat (2002), The relevant time scales in estimating the air–sea CO_2 exchange in a mid-latitude region, *Deep Sea Res. Part II*, *49*(11), 2067–2092.

Monteiro, P. M. S., et al. (2010), A global sea surface carbon observing system: Assessment of changing sea surface CO_2 and air-sea CO_2 fluxes, in *Proceedings of the "OceanObs'09: Sustained Ocean Observations and Information for Society" Conference*, edited by J. Hall, D. E. Harrison, and D. Stammer, ESA Publ. WPP-306, Venice, Italy, doi:10.5270/OceanObs09.cwp.64, 21–25 Sept.

Nightingale, P. D., G. Malin, C. S. Law, A. J. Watson, P. S. Liss, M. I. Liddicoat, J. Boutin, and R. C. Upstill-Goddard (2000), In situ evaluation of air-sea gas exchange parameterizations using novel conservative and volatile tracers, *Global Biogeochem. Cycles*, *14*(1), 373–387, doi:10.1029/1999GB900091.

Pfeil, B., et al. (2013), A uniform, quality controlled Surface Ocean CO_2 Atlas (SOCAT), *Earth Syst. Sci. Data*, *5*, 125–143, doi:10.5194/essd-5-125-2013.

Resplandy, L., J. Boutin, and L. Merlivat (2014), Observed small spatial scale and seasonal variability of the CO_2-system in the Southern Ocean, *Biogeosciences*, *11*, 75–90, doi:10.5194/bg-11-75-2014.

Rödenbeck, C., R. F. Keeling, D. C. E. Bakker, N. Metzl, A. Olsen, C. Sabine, and M. Heimann (2013), Global surface-ocean pCO_2 and sea–air CO_2 flux variability from an observation-driven ocean mixed-layer scheme, *Ocean Sci.*, *9*, 193–216, doi:10.5194/os-9-193-2013.

Sabine, C. L., et al. (2004), The oceanic sink for anthropogenic CO_2, *Science*, *305*(5682), 367–371, doi:10.1126/science.1097403.

Sabine, C. L., et al. (2013), Surface Ocean CO_2 Atlas (SOCAT) gridded data products, *Earth Syst. Sci. Data*, *5*, 145–153, doi:10.5194/essd-5-145-2013.

Sutton, A. J., et al. (2014), A high-frequency atmospheric and seawater pCO_2 data set from 14 open ocean sites using a moored autonomous system. Open access, *Earth Sys. Sci. Data*, *6*, 353–366, doi:10.5194/essd-6-353-2014.

Swart, S., S. J. Thomalla, and P. M. S. Monteiro (2014), The seasonal cycle of mixed layer dynamics and phytoplankton biomass in the Sub-Antarctic Zone: A high-resolution glider experiment, *J. Mar. Syst.*, doi:10.1016/j.jmarsys.2014.06.002.

Takahashi, T., et al. (2009), Climatological mean and decadal change in surface ocean pCO_2, and net sea-air CO_2 flux over the global oceans, *Deep Sea Res., Part II*, *56*, 554–577.

Takahashi, T., C. Sweeney, B. Hales, D. Chipman, T. Newberger, J. Goddard, R. Iannuzzi, and S. Sutherland (2012), The changing carbon cycle in the Southern Ocean, *Oceanography*, *25*(3), 26–37.

Thomalla, S. J., N. Fauchereau, S. Swart, and P. M. S. Monteiro (2011), Regional scale characteristics of the seasonal cycle of chlorophyll in the Southern Ocean, *Biogeosciences*, *8*(10), 2849–2866, doi:10.5194/bg-8-2849-2011.

Wanninkhof, R., et al. (2013), Global ocean carbon uptake: Magnitude, variability and trends, *Biogeosciences*, *10*, 1983–2000, doi:10.5194/bg-10-1983-2013.